Theoretical and Computational Analysis on Blunt Shaped Reentry Capsule

Chaithanya.T, Bachu Anusha, Manikandan.S

Abstract—For high aerodynamic drag and safe returning of capsule on the earth, to protect astronaut from radiation, the blunt shape reentry capsule is required. The flow fields over the blunt shaped reentry capsule are numerically obtained by the steady state, axisymmetric, compressible Navier–Stokes k-□ turbulence model for free stream mach numbers are in the range of 2 and 4. Employing a finite volume approach which reduces the governing equations to semi-discretized ordinary differential equations. The numerical simulation is carried out on a structural grid. The flow field features around reentry capsule, such as bow shock, sonic line, expansion are obtained. A good agreement is found between the computationally calculated value of aerodynamic drag co-efficient blunt shape reentry capsule with the theoretical value. The effects of geometrical parameters, blunt shapes have been numerically investigated for various reentry configurations which will be useful for forming the strong shock wave in supersonic flow, as a result there is a increases in aerodynamic drag during landing of the vehicle.

Index Terms— blunt , reentry capsule, supersonic flows, drag

I. INTRODUCTION

Reentry of the vehicle into earth's atmosphere is the movement of an object into and through the gases of planet's atmosphere from outer space. When the reentry vehicle past with high velocity towards the earth's atmosphere due to velocity differences, it generates a shock near the capsule and heat load. Due to the production of heat it causes structural damage of the vehicle, improper landing, sometimes it leads to harmful to crew members also.To eradicate these problems, blunt shape of the reentry vehicle discovered in 1951 by the H. Julian Allen and A. J. Eggers. Jr of the National Advisory Committee for Aeronautics(NACA).The blunt shape made the most effective heat shield. Allen and Eggers showed that the heat load experienced by the entry vehicle was inversely proportional to the drag co-efficient. i.e. greater drag, less the heat load. Making the reentry vehicle in blunt, air cannot get out of the way quickly enough, and acts as air cushion to push shock wave and heated shock layer from vehicle. Since most of hot gases are no longer in direct contact with the vehicle. Making the vehicle in blunt shape, when it entering into earth atmosphere in supersonic speed, generates a bow shock wave, which causes a rather high surface pressure and as a result of high aerodynamic drag which is also require for aerobraking purposes. Highly blunt configurations are generally preferred to decelerate space capsule for safe returning on earth's atmosphere. Bow shock is detached from blunt fore-body and is having a mixed subsonic-supersonic region between them.

Manuscript received March 2014.

Ms.T.Chaithanya, UG Final Year Student, Department of Aeronautical Engineering, Jeppiaar Engineering College, Chennai, India,

Ms.Bachu Anusha, UG Final Year Student, Department of Aeronautical Engineering, Jeppiaar Engineering College, Chennai, India.

Mr.S.Manikandan, Assistant Professor, Department of Aeronautical Engineering, Jeppiaar Engineering College, Chennai, India.

Reentry capsule configurations significantly differ from each other due to entry conditions, trajectory and a number of aerodynamic factors such as aerodynamic axial force, normal force, static moment and damping coefficients. This leads to the necessity to investigate the influence of the shape of blunted body on the flow field and aerodynamic characteristics. The flow analysis and shock formation have been carried out by solving Navier-Stokes turbulence model by using ANSYS FLUENT. The upwind, implicit, second order accurate scheme of ALGORITHM is used. Aerodynamic heating and pressure along with the fore body during atmospheric entry of capsule have been computed by (Hass and Venkatapathy, 1995) using an available general atmospheric simulation program.

II. COMPUTATIONAL APPROACH

The analysis of the flow on reentry capsule at mach 2 and 4 are proved with the theoretical calculation. The analysis should be done by FLUENT and GAMBIT on four blunt models. In the given below figures we have clearly find the shock angle, drag coefficient, flow separation angle, mach drop and distance between the shock for the different blunt capsule.

III. GEOMETRICAL CONFIGURATIONS

For the conical shape blunt capsule radius 0.99m, diameter 1.98m and length 1.50m. For the spherical shape blunt capsule radius o.99m, diameter 1.98m, and length 1.19m. For the elliptical blunt shape capsule radius 0.99m, corner radius 0.2m, diameter. 1.98 m, and length 1.5m. For the flat blunt shape reentry capsule radius 1.2m, diameter 2.4m and length 1.29m.

A. Figures and tables

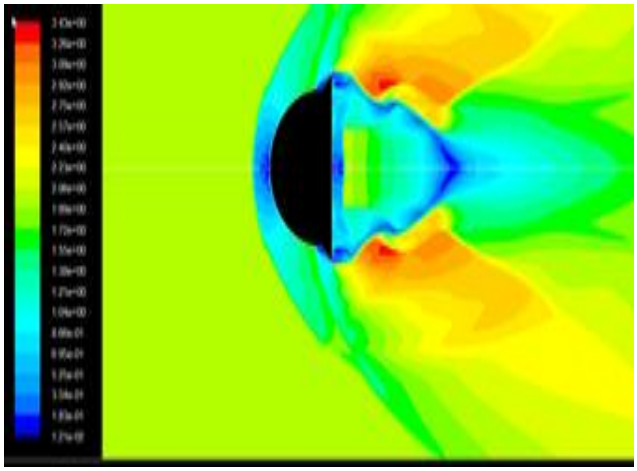

Fig.1. Flow analysis on Spherical blunt body at mach 2

Published By:
Blue Eyes Intelligence Engineering
& Sciences Publication Pvt. Ltd.

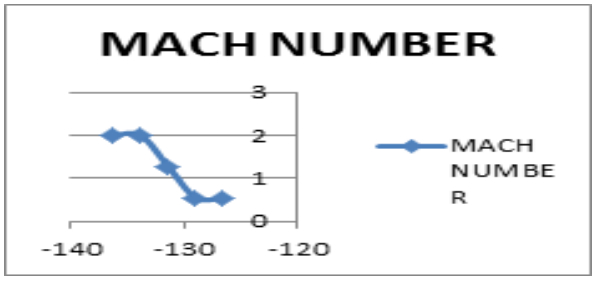

Graph.1.Mach drop on Spherical blunt body at mach 2

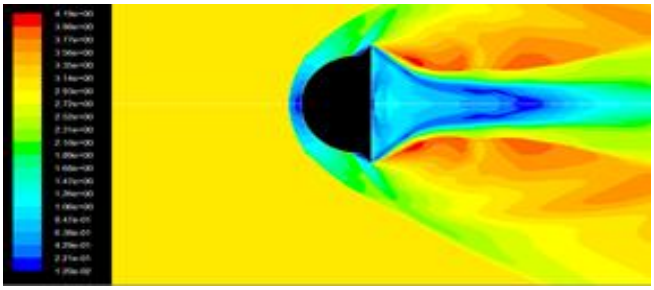

Fig.2. Flow analysis on Spherical blunt body at mach 4

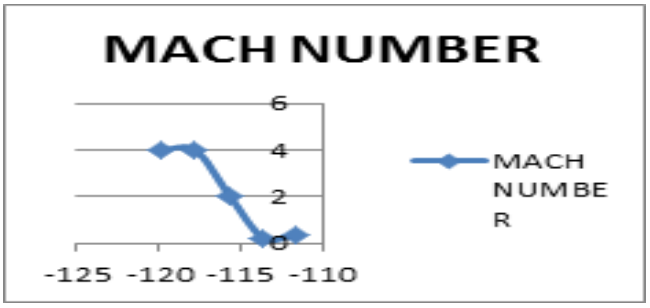

Graph.2.Mach drop on Spherical blunt body at mach 4

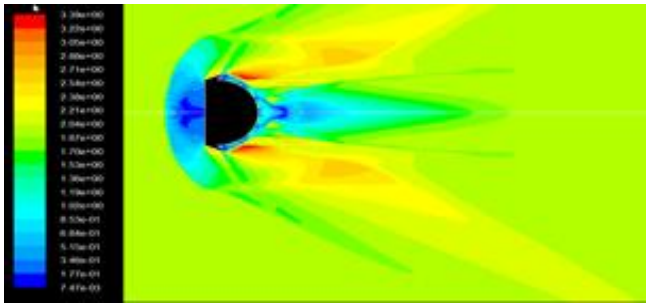

Fig.3. Flow analysis on Flat spherical blunt body at mach 2

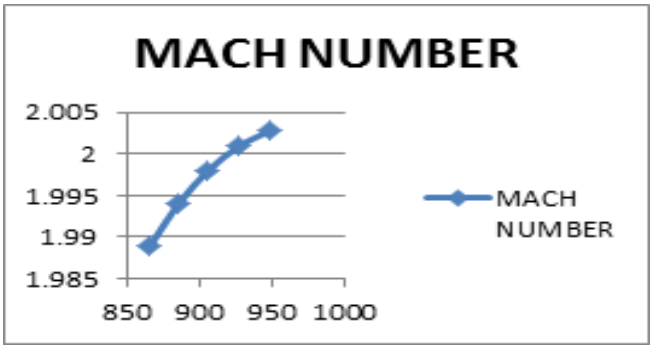

Graph.3.Mach drop on Flat spherical blunt body at mach 2

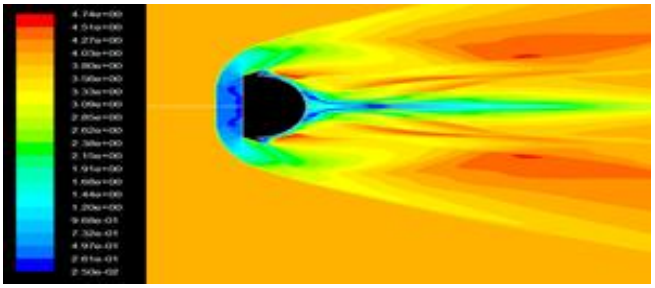

Fig.4. Flow analysis on Flat Spherical blunt body at mach 4

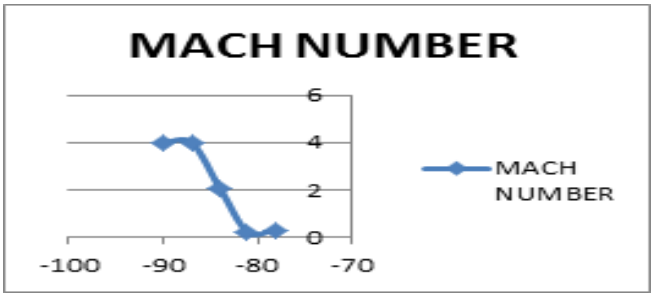

Graph.4.Mach drop on Flat spherical blunt body at mach 4

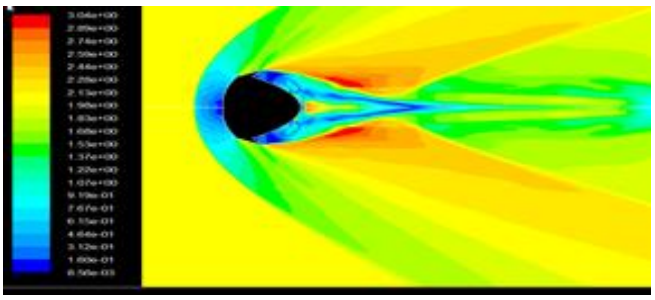

Fig.5. Flow analysis on Elliptical blunt body at mach 2

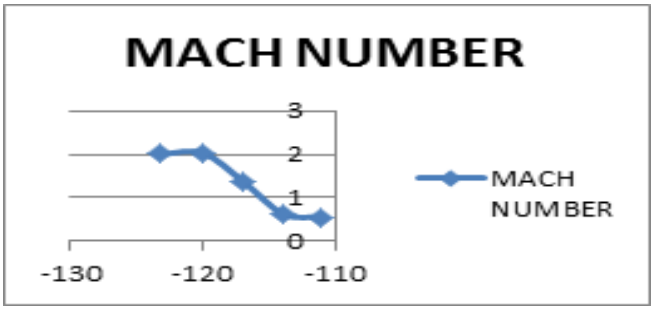

Graph.5.Mach drop on Elliptical blunt body at mach 2

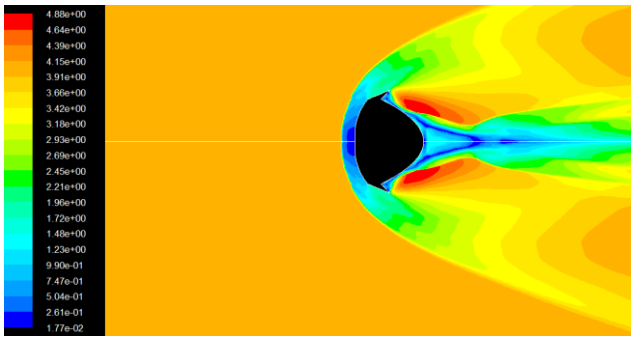

Fig.6. Flow analysis on Elliptical blunt body at mach 4

Published By:
Blue Eyes Intelligence Engineering
& Sciences Publication Pvt. Ltd.

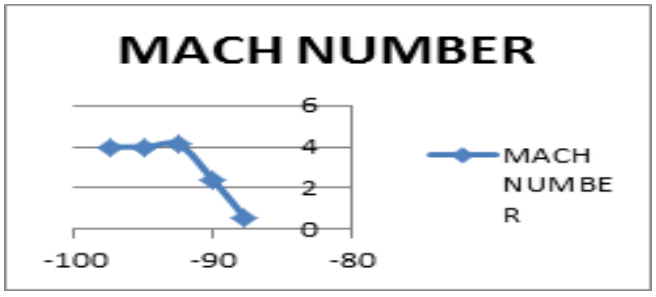

Graph.6.Mach drop on Elliptical blunt body at mach 4.

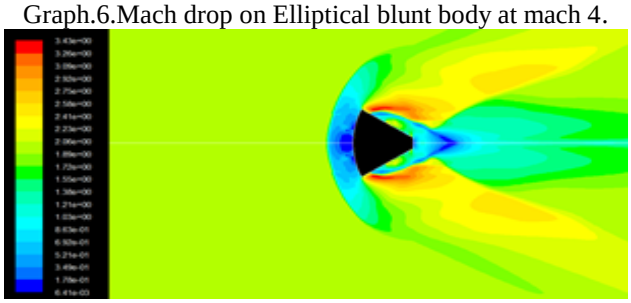

Fig.7. Flow analysis on conical blunt body at mach 2

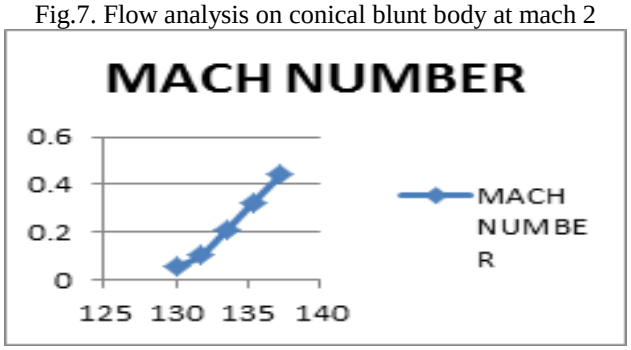

Graph.7.Mach drop on Conical blunt body at mach 2

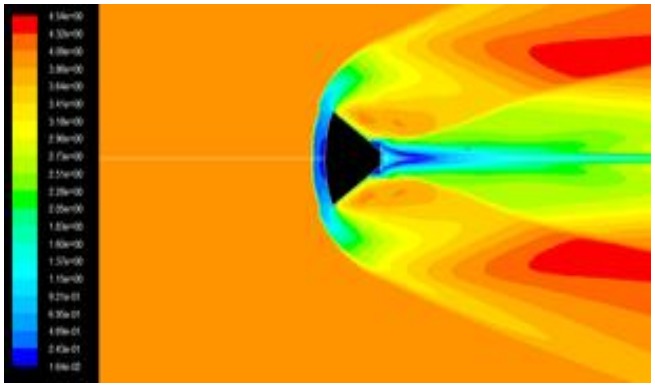

Fig.8. Flow analysis on conical blunt body at mach 4

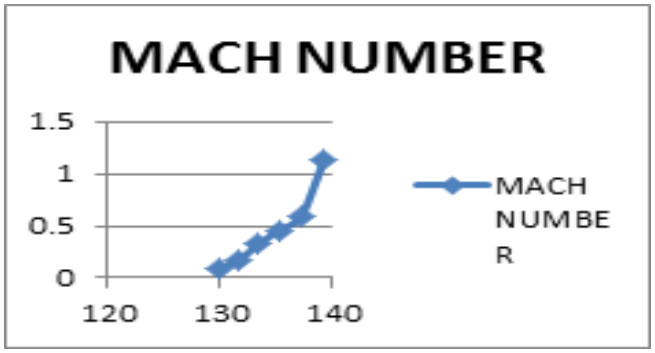

Graph.8.Mach drop on Conical blunt body at mach 4

B. Tabular column

FLOW TYPE	MACH NUMBER	
	DROP	RISE
Spherical shape body at mach 2	1.36566	2.01109
Spherical shape body at mach 4	2.42707	3.9977
Flat blunt shape at mach 2	1.41595	2.00394
Flat blunt shape at mach 4	2.46733	3.99697
elliptical blunt body at mach 2	1.26877	1.14879
Elliptical blunt body at mach 4	2.04091	108294
Conical blunt shape at mach 2	0.054413	0.101679
Conical blunt shape at mach 4	0.096359	0.175176

IV. DRAG COEFFICIENT

Drag coefficient obtained computationally in fluent software package at mach 2, 4 on four blunt shape bodies are given below.

zone name	total coefficient
wall	1.7198097
net	1.7198097
wall	1.6568713
net	1.6568713

[1].Drag coefficient of conical shape blunt at mach 2, 4

zone name	total coefficient
wall	1.5570588
net	1.5570588
wall	1.2705941
net	1.2705941

[2].Drag coefficient of spherical blunt body at mach 2, 4

zone name	total coefficient
wall	1.0902731
net	1.0902731
wall	1.1695118
net	1.1695118

[3].Drag coefficient of flat spherical body at mach 2, 4

Published By:
Blue Eyes Intelligence Engineering
& Sciences Publication Pvt. Ltd.

zone name	total coefficient
wall	1.6789772
net	1.6789772
wall	1.602784
net	1.602784

[4].Drag coefficient of elliptical body at mach 4, 2

V. SHOCK ANGLE

Shock and flow angle is obtained from flow analyzed in software package (ANSYS FLUENT).

Blunt shape models	Shock angle(β)	
	Mach 2	Mach 4
Conical shape body	77°	81°
Spherical shape body	81.5°	82°
Elliptical shape body	75°	77°
Flat blunt shape body	75°	80°

VI.SHOCK DISTANCE

The distance between the shock and model is measured by taking 5:2 ratio of diameter of the model and distance of the shock by using ruler.

Model	Distance (Δ*f*)(cm)	
	Mach 2	Mach 4
Conical shape body	3.5	1.8
Spherical shape body	1.7	1
Elliptical shape body	3	1.8
Flat blunt shape body	5.4	3.2

VII. COMPUTATIONAL RESULT

Blunt bodies	Mach drop		Drag coefficient		Shock angle(β)		Distance (Δ*f*)(m)	
	M 2	M 4	M 2	M 4	M 2	M 4	M 2	M 4
Conical	0.054	0.096	1.719	1.65	77^0	81^0	3.5	1.8
Spherical	1.365	2.42	1.557	1.27	81.5^0	82^0	1.7	1
Elliptical	1.268	2.040	1.68	1.60	75^0	77^0	3	1.8
Flat	1.415	2.467	1.09	1.16	75^0	80^0	5.4	3.2

VIII. THEORITICAL APPROACH

When an oblique shock is likely to form at an angle which can not remain on the surface, a nonlinear phenomenon arises where the shock wave will form a continuous pattern around the body. These are termed bow shocks because of this reason we are using oblique shock relations in bow shock. The theoretical calculation is done by θ-β-M relation, to find shock angle and mach drop.

$$\tan\theta = 2\cot\beta\frac{M_1^2\sin^2\beta - 1}{M_1^2(\gamma + \cos 2\beta) + 2}$$

For example:
Finding for spherical blunt body:
Flow deflection angle:

Tan θ = 2 cot β (M^2_1 $\sin^2$ β -1/M_1 ^{2} (ɾ + cos 2β) +2)
= 2 cot β ($(2)^2$ $\sin^2$ (18.5)-1/ $(2)^2$ (1.4 + cos (2x 81.5))+2)
= tan-□((2/tan 81.5)(0.7714))
θ = 12.98^0

Mach drop**:**

Mn_2 = M_2 sin β
M_2 = Mn_2 /sin β
Mn_2 /sin β = (1+((ɾ -1)/2)M_1 ^{2})/ɾ M_1 ^{2}-((ɾ - 1)/2))½
Mn_2 /sin 8.15^0 = 0.57=> M_2 = 0.576

Distance (Δ*f*):

On 1951 **Hayer** and **probstin** proposed that where the shock detachment distance decrease with increasing the density ratio. The equation expressed as,

Δ□/Ds= 2.8(ρ/ρ□) ½

□=ρ/ρ□ = ((ɾ -1)M □² +2)/(ɾ +1)M □²)
= ((0.4)$(2)^2$+2/(2.4)$(2)^2$)
= 176.199 cm
= 1.7 m

IX. CONCLUSION

Finally when we compare the values obtained for four blunt shape bodies computationally, conical blunt body have more drag coefficient 1.719, strong shock angle 77, high Mach drop 0.0544 and less shock distance 3.5 m. From this we can conclude that conical blunt shape body is more efficient than all other blunt shape bodies and theoretically have been proved. Hence there is a good agreement found between theoretical approach and computational approach.

REFERENCES

[1] Lee, D.B., Bertin, J.J. and Goodrich, W.D., "Heat Transfer Rate and Pressure Measurements Obtained During Apollo Orbital Entries", NASA TN D-6028, October 1970.

[2] Lee, D.B., "Apollo Experience Report: Aerothermodynamics Evaluation", NASA TN D-6843, June 1972.

[3] Hillje, E., "Entry Flight Aerodynamics from Apollo Mission AS-202", NASA TN D-4185, October 1967.

[4] Wright, M.J., Prabhu, D.K. and Martinez, E.R., "Analysis of Afterbody Heating Rates on the Apollo Command Modules, Part 1", Journal of Thermophysics and Heat Transfer, Vol. 20, No. 1, pp. 16-30, 2006.

[5] Walpot, L., "Development and Application of a Hypersonic Flow Solver", Ph.D. Thesis, T.U. Delft University, May 2002.

[6] Gerhold, T.O., Friedrich, J.E. and Galle, M., "Calculation of Complex Three-Dimensional Configurations Employing the DLR-TAU-Code", 16th Aerospace Sciences Meeting, Reno, NV, USA, AIAA Paper 97-0167, January 1997

[7] Walpot, L.M.G., Noeding, P., Tarfeld, F., Molina, R.C., Gülhan, A. and Paulat, J.-C., "Transonic and Supersonic Static Stability Analysis of the CARV Reentry Vehicle", 14th AIAA/AHI Space Planes and Hypersonic Systems and Technologies Conference, AIAA Paper 2006-8077, 2006.

[8] Lee, D.B., Bertin, J.J. and Goodrich, W.D., "Heat Transfer Rate and Pressure Measurements Obtained During Apollo Orbital Entries", NASA TN D-6028, October 1970.

Published By:
Blue Eyes Intelligence Engineering
& Sciences Publication Pvt. Ltd.